Information Fusion 96 (2023) 252–268

Contents lists available at ScienceDirect

Information Fusion

journal homepage: www.elsevier.com/locate/inffus

Epilepsy detection in 121 patient populations using hypercube pattern from EEG signals

Irem Tasci [a], Burak Tasci [b], Prabal D. Barua [c,d,e,f,g,h,i,j,k], Sengul Dogan [l], Turker Tuncer [l], Elizabeth Emma Palmer [m,n], Hamido Fujita [o,p,q], U. Rajendra Acharya [r,*]

[a] Department of Neurology, School of Medicine, Firat University, Elazig, 23119, Turkey
[b] Vocational School of Technical Sciences, Firat University, Elazig, 23119, Turkey
[c] Cogninet Australia, Sydney, NSW, 2010, Australia
[d] School of Business (Information System), University of Southern Queensland, Australia
[e] Faculty of Engineering and Information Technology, University of Technology Sydney, Sydney, NSW, 2007, Australia
[f] Australian International Institute of Higher Education, Sydney, NSW, 2000, Australia
[g] School of Science & Technology, University of New England, Australia
[h] School of Biosciences, Taylor's University, Malaysia
[i] School of Computing, SRM Institute of Science and Technology, India
[j] School of Science and Technology, Kumamoto University, Japan
[k] Sydney School of Education and Social work, University of Sydney, Australia
[l] Department of Digital Forensics Engineering, College of Technology, Firat University, Elazig, Turkey
[m] Centre of Clinical Genetics, Sydney Children's Hospitals Network, Randwick, 2031, Australia
[n] School of Women's and Children's Health, University of New South Wales, Randwick, 2031, Australia
[o] Faculty of Information Technology, HUTECH University, Ho Chi Minh City, Viet Nam
[p] Andalusian Research Institute in Data Science and Computational Intelligence, University of Granada, Granada, Spain
[q] Regional Research Center, Iwate Prefectural University, Iwate, Japan
[r] School of Mathematics, Physics and Computing, University of Southern Queensland, Springfield, Australia

ARTICLE INFO

Keywords:
Hypercube pattern
Feature fusion
Feature selection
Epilepsy detection
Fusion-based feature engineering

ABSTRACT

Background: Epilepsy is one of the most commonly seen neurologic disorders worldwide and has generally caused seizures. Electroencephalography (EEG) is widely used in seizure diagnosis. To detect epilepsy automatically, various machine learning (ML) models have been introduced in the literature, but the used EEG signal datasets for epilepsy detection are relatively small. Our main objective is to present a large EEG signal dataset and investigate the detection ability of a new hypercube pattern-based framework using the EEG signals.

Material and method: This study collected a large EEG signal dataset (10,356 EEG signals) from 121 participants. We proposed a new information fusion-based feature engineering framework to get high classification performance from this dataset. The dataset consists of 35 channels, and our proposed feature engineering model extracts features from each channel. A new hypercube-based feature extractor has been proposed to generate two feature vectors in the feature extraction phase. Various statistical parameters of the signals have been used to create a feature vector. Multilevel discrete wavelet transform (MDWT) has been applied to develop a multileveled feature extraction function, and seven feature vectors have been extracted. In this work, we have extracted 245 ($=35 \times 7$) feature vectors, and the most valuable features from these vectors have been selected using the neighborhood component analysis (NCA) selector. Finally, these selected features were fed to the k nearest neighbors (kNN) classifier with the leave one subject out (LOSO) cross-validation (CV) strategy. These results have been voted/fused to obtain the highest classification performance.

Results: In this work, we have attained 87.78% classification accuracy using voting these vectors and 79.07% with LOSO CV with the EEG signals.

Conclusions: The proposed fusion-based feature engineering model achieved satisfactory classification performance using the largest EEG signal datasets for epilepsy detection.

* Corresponding author.
E-mail address: Rajendra.Acharya@usq.edu.au (U.R. Acharya).

https://doi.org/10.1016/j.inffus.2023.03.022
Received 23 January 2023; Received in revised form 27 March 2023; Accepted 30 March 2023
Available online 31 March 2023

1. Introduction

Epilepsy is a neurological disease characterized by epileptic seizures, which are recurrent, recurrent abnormal, paroxysmal, excessive, or synchronized neuronal activities in the central nervous system. A broad range of etiologies and marked variability in clinical outcomes are associated with epilepsy. Still, the global burden of epilepsy is immense, with over 45 million people affected by active epilepsy [1]. According to the definition revised by the International Association to Combat Epilepsy (ILAE) in 2014, epilepsy is a disease of the brain defined by any of the following conditions (i) the presence of at least two unprovoked seizures occurring at least twenty-four hours apart, or (ii) one unprovoked (or reflex) seizure and a probability of further seizures similar to the general recurrence risk after two unprovoked seizures, or (iii) the diagnosis of any epilepsy syndrome [2]. After diagnosing epilepsy, the type of seizure must be determined. The ILAE continually revises the operational classification of seizure types and epilepsy syndromes. In the most current classification, seizure types can be focal, generalized, or unknown onset, with subcategories for focal seizures of motor, non-motor, and retained or impaired awareness. After the seizure type is diagnosed, clinical etiological findings and EEG features should be considered [3]. A syndromic diagnosis, where possible, is frequently important to guide clinical management and provide insights into prognosis. For example, some syndromes may start or remit at certain ages, and others may be correlated with a range of intellectual, psychiatric, and other comorbidities [4].

A full evaluation for epilepsy requires a combination of careful clinical history, physical examination, EEG, and, in many cases, neuroimaging [5]. EEG is still the most important laboratory test in the diagnosis of epilepsy, although a normal EEG cannot exclude an epilepsy diagnosis [6]. In addition, EEG can enable the diagnosis of epilepsy, the recording of seizure activity, the follow-up of epilepsy patients, and the differentiation of subtypes of epilepsy syndromes that begin in childhood [7].

While epileptic discharges such as spike, sharp, and spike-wave complexes expressing epileptic activity in EEG originate from a small region called epileptic focus in focal epilepsies. If epileptic discharges originate synchronously from both hemispheres and cannot be localized to a single focus is named generalized epilepsy [7,8]. The average detection rate of epileptic activity using the first routine EEG signals obtained after the first seizure is 29% (the detection range is from 8% to 50%) [9]. Moreover, a sleepless EEG test is recommended to detect epileptic discharges in an additional 13–35% of individuals. [10]. If diagnostic uncertainty remains, longer-term ambulatory EEG or inpatient video-EEG monitoring may be requested to maximize the detection of epileptic activity and ideally correlate with clinical events [11].

EEG records ictal (seizure) and interictal (between seizures) activities and can also be used in the follow-up of epilepsy patients to gage response to treatments and guide management [8].

EEG signals essentially provide a ‘read out’ of the brain’s electrical activity and can show changes in the brain’s electrical activity over time [12]. In this respect, EEG is used as an important diagnostic method in determining the differences in the neural activities of healthy individuals according to the neural activities of patients with epilepsy [13]. However, interpreting EEG signals requires highly skilled expertise, and neurologists can have difficulty interpreting EEGs. Moreover, there is a global shortage of trained specialists in EEG interpretation [14]. Machine learning or deep learning models are increasingly being used to classify EEG signals to overcome these challenges [15–17]. Recent artificial intelligence studies in the literature on detecting epilepsy using EEG signals are listed below.

Assali et al. [18] applied Multivariate Autoregressive Model (MVAR), sample entropy, and Short-Time Fourier Transform (STFT) preprocessing to the CHB-MIT dataset. They used a 1D-convolutional neural network (CNN) in their proposed method. They reported 90.10% accuracy and 88.60% sensitivity for their study. Cimr et al. [19] detected automatic seizures using the Bonn and CHB-MIT EEG datasets. They presented a customized deep CNN with eight layers, and 98.00% classification accuracy was obtained using the Bonn EEG dataset. Moreover, they yielded 96.99% in the CHB-MIT dataset. Sheoran et al. [20] recommended a scalogram extraction-based EEG classification model with a local binary pattern (LBP). They attained 99.08% with the support vector machine (SVM) classifier. Li et al. [21] classified epilepsy with an empirical mode decomposition (EMD) and common spatial pattern (CSP) based method. The CHB-MIT dataset. They obtained accuracy, specificity, and sensitivity of 97.49%, 97.50%, and 97.34%, respectively, with the SVM classifier. Usman et al. [22] preprocessed it with EMD. The handcrafted features and CNN-based features were used to extract features, and they selected the extracted features with Pearson Correlation Coefficient (PCC) and Particle Swarm Optimization (PSO). They obtained 96.28% sensitivity, 96.05% accuracy, and 95.65% specificity in the CHB-MIT dataset using Model Agnostic Meta-Learning (MAML) classifier. Ryu et al. [23] transformed EEG data into a time-frequency domain using Discrete Wavelet Transform (DWT). They predicted epileptic seizures with a hybrid model of DenseNet and Long Short-Term Memory (LSTM). They obtained 93.28% prediction accuracy, 92.92% sensitivity, and 93.65% specificity with the CHB-MIT dataset. Goshvarpour et al. [24] proposed a hybrid method of the Walsh-Hadamard transform and Hilbert transform (HTFWHT) to predict epileptic patients. Using the Bonn dataset, they reported 100% accuracy with a probabilistic neural network (PNN) classifier. Khan et al. [25] presented a frequency transformation and statistical feature extraction-based EEG signal classification model to detect epileptic EEG signals automatically. They used two epilepsy dataset and their proposal yielded 96.00% accuracy for the Bonn dataset and 83.30% for the SNRL dataset. Mishra et al. [26] proposed a method based on DWT and moth flame optimization for epilepsy detection. Using the Bonn dataset, they obtained 96.00% accuracy, 95.00% specificity, and 94.00% f-score with the DWT and moth flame optimization-based extreme learning machine classification method. Amiri et al. [27] suggested an EEG classification model based on sparse common spatial patterns (sCSP) and adaptive STFT. They reported 98.81% accuracy and 99.19% sensitivity using the CHB-MIT epileptic EEG dataset. Kumar et al. [28] used the variable mode decomposition (VMD) method to decompose the quasi-orthogonal signal in the EEG signals. Then, statistical values such as differential entropy (DE) and mean square rate peak size (PRMS) were calculated by applying semantic feature extraction. They achieved 94.10% accuracy with the Random Forest classifier. Zarei et al. [29] detected automatic epileptic seizures using DWT and orthogonal matching pursuit (OMP) methods. They obtained average accuracy, specificity, and sensitivity of 97.09%, 97.26%, and 96.81%, respectively, with the DWT-based method and the SVM classifier. Rashed-Al-Mahfuz et al. [30] aimed to use power of the CNNs. Hence, they presented a spectrogram extraction-based EEG classification model. They reached the highest accuracy rate of 99.21% with the VGG16 models. However, their model is time-consuming, and they used random separation-based validation. Shen et al. [31] used CNN and tunable-Q wavelet transforms for epilepsy disease detection using the CHB-MIT dataset. Their approach aimed to detect epilepsy and achieved an accuracy of 97.57%. Zhao et al. [32] presented an epileptic seizure detection method using EEG signals with CHB-MIT and Siena scalp EEG datasets. Their method was based on CNN and transformer methods and attained an accuracy of 98.76%. Qiu et al. [33] proposed a method to detect epilepsy using residual neural networks and LSTM. They reported an accuracy of 90.17% for the classification of five classes using the Bonn EEG dataset. Poorani and Balasubramanie [16] proposed an approach to predict an epileptic seizure using CNN and LSTM methods. They reported an accuracy of 94.48%. Mir et al. [34] developed a seizure detection model using a hybrid deep network and they used autoencoder and bidirectional long short memory together. They attained an accuracy of 99.80% using CHB-MIT dataset.

1.1. Literature gaps

The main research gaps in detecting epilepsy using EEG signals are as follows:

- There are few epilepsy detection EEG signal datasets available. But these datasets are relatively small.
- To the best of our knowledge, this is the first fusion-based feature engineering model developed for EEG epilepsy detection.
- Deep learning models are popular since they yield high classification capability but are expensive. In this work, we have presented a new feature engineering framework.
- There is a limited number of methods using LOSO CV.

1.2. Motivation and our model

Epilepsy is one of the most commonly seen neurological conditions globally. Accurate epilepsy detection is critical for prompt and appropriate management and prognostication [35,36]. EEGs are widely used to diagnose epilepsy, but manual interpretation using EEG signals is challenging and requires specific training [37]. Machine learning, therefore, is an excellent enabling technology to improve epilepsy diagnosis with growing research on artificial intelligence and optimization [38,39]. Most of the datasets used to date are small, and the results obtained from these datasets cannot be generalized. Moreover, random separation-based validation techniques have been used, resulting in unreliable results [40]. We collected a huge dataset containing more than 10,000 EEG signals to overcome these gaps. Moreover, we have used Leave-One-Out Cross-Validation (LOSO CV) to ensure reliable results. Our essential motivation is to propose a highly accurate fusion-based feature engineering model to optimize clinical diagnosis and classification of epilepsy, with the potential to improve patient outcomes.

Our model contains fused multiple feature vector generation, feature dimension reduction, classification with LOSO CV, and majority voting phases. Hence, it is an information fusion model. In the feature extraction phase, we extracted features from each channel. We have used multilevel discrete wavelet transform (MDWT) [41] to generate features and create wavelet bands. We have extracted features from wavelet bands and the original EEG signal. Herein, we have suggested a new textural feature generation function named hypercube pattern since we have used a hypercube shape to create this feature extraction function. This feature extraction function generates three feature vectors by using the edges of the hypercube. The features of the hypercube pattern and statistical features have been fused in this work. Seven feature vectors have been extracted using these combinations. There are 35 channels in the collected dataset. 245 (35×7) feature vectors are created, and the most discriminative features have been selected by neighborhood component analysis (NCA) [42]. The selected features have been considered as input to the k-nearest neighbors algorithm (kNN) [43] with the LOSO CV strategy (121 subjects). Therefore, it can be called a 121-fold CV (without random separation). The calculated 245 predicted label vectors have been voted, and the best classification result is selected.

1.3. Theoretical background

Advanced signal processing (ASP) is one of the important research areas used to extract valuable features from physiological signals to develop accurate models. Using ASP models, feature engineering models have been created [44]. Moreover, graph-based models are valuable and effective for machine learning [45–47]. Therefore, we have presented a new graph-based feature extractor by using hypercube. In this aspect, we have presented a hypergraph-based feature extraction function. This feature extractor generates three textural feature vectors. Using these three feature vectors and statistical features (we have used statistical features as salt and added them), 7 ($=2^3-1$) feature vectors have been created. In this work, the best pattern has been selected for each channel. Iterative majority voting (IMV) is used to develop an ensemble model.

1.4. Contributions

The contributions of the presented model are listed below.

- Many machine-learning methods have been proposed for automatic epilepsy detection. However, a limited number of big public EEG signal datasets are available in the literature. Hence, we have collected a huge dataset and proposed an accurate epilepsy detection model. To the best of our knowledge, our gathered EEG signal dataset is one of the biggest epilepsy datasets used for automated epilepsy detection.
- A new graph-based feature generation function has been proposed using a hypercube shape as a pattern. Three directed graphs have been obtained using this pattern to generate features. Therefore, we generated three feature vectors using the recommended hypercube pattern.
- We have presented a new information fusion-based feature engineering model to get high classification performance. Our proposed model generates 488 (=245 non-voted + 243-voted results) results and selects the best (prediction vector with the highest accuracy) out of 488 vectors. Hence, our model is self-organized.

2. Material and method

This section details the collected dataset and the presented hypercube pattern-based feature engineering architecture.

2.1. Dataset

Data were gathered from 35 channels using a 10–20 EEG electrode position system with a sampling frequency of 500 Hz. The dataset consists of EEG signals of control and epilepsy patients. Fig. 1 shows the signal sample of all channels of the control and epilepsy patients. The channels used in this work are parietal (P), temporal (T), frontal (F), occipital (O), frontopolar (Fp), central (C), and auricular (A). The even number of channels represents the right hemisphere, and the odd numbers of channels represent the left hemisphere. Participants under 18 years were not included in the study. Generalized epileptic activity was observed in all channels in the traces of the patients included in the study. Patients with focal epileptic activity were not included in the study. The demographic properties of the participants used to gather EEG signals in the study are listed in Table 1.

As can be seen from Fig. 1, this dataset contains 35 channels. The details of these channels are listed in Table 2.

2.2. Hypercube pattern

We recommended a new textural feature creation function in this work, and this feature extraction function uses a hypercube graph to generate features. The proposed hypercube pattern is a histogram-based feature extractor. Data block, directed graph, and signum function have been used to generate binary features. The map signals have been generated using the extracted bits by deploying binary to decimal conversion. Finally, the histogram extraction function has been applied to the created map signals, and the extracted histograms have been used as a feature vector. The general schematic demonstration of the presented hypercube pattern is depicted in Fig. 2.

Map coding defines the binary-to-decimal conversion, and the generated signals are named map signals in this figure. We have used three-bit groups. Therefore, three map signals have been generated, representing each pattern. The map signals are feature signals. The

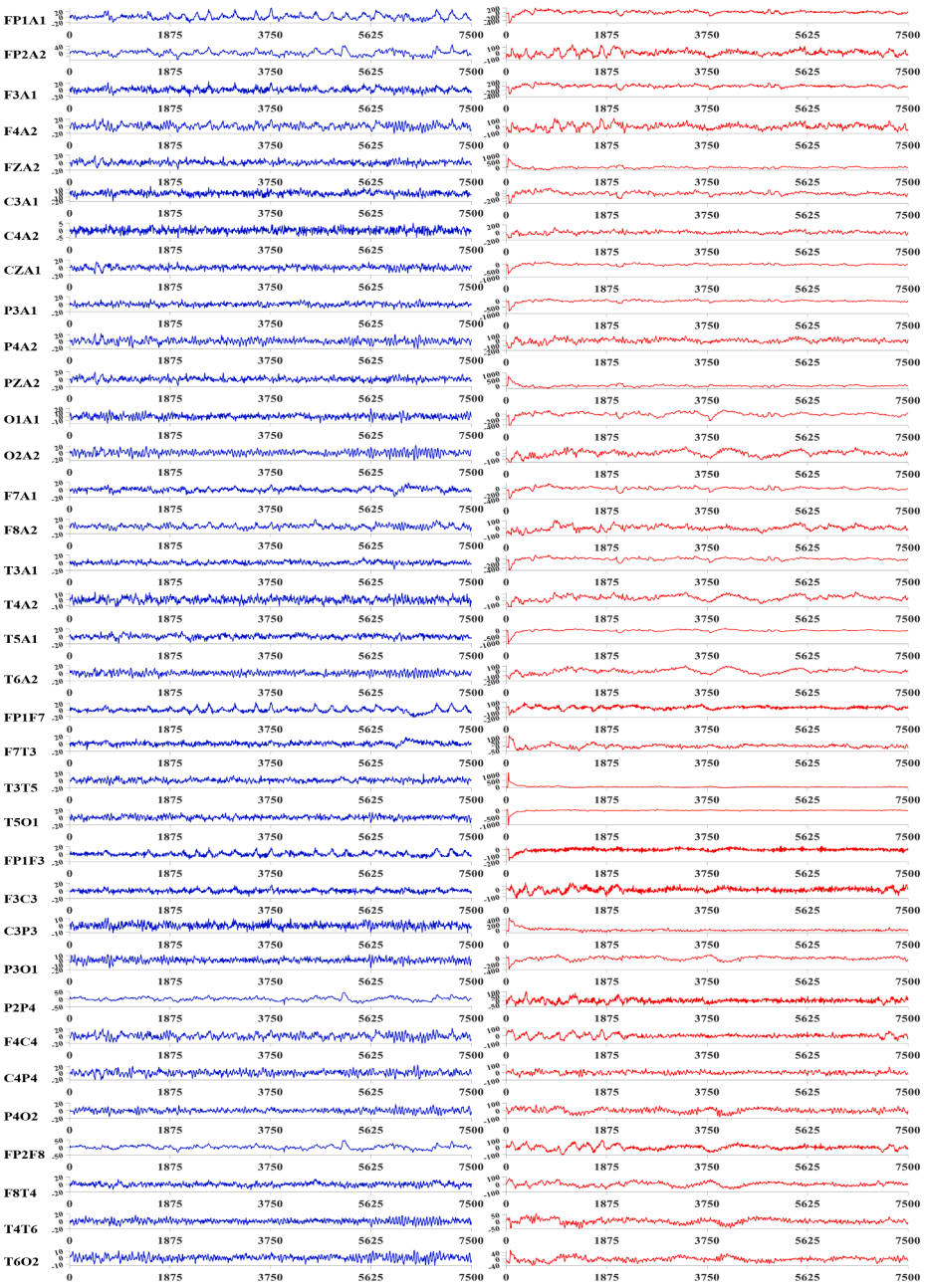

Fig. 1. Typical EEG signals of 35 channels of a healthy subject.

Table 1
Information of participants.

Class	Healthy Control		Epilepsy	
Sex	Female(n = 36)	Male(n = 35)	Female(n = 27)	Male(n = 23)
Mean Age±sd, years	33.94±14.13	39.77 ±21.83	38.77±18.13	40.43 ±19.07
Age range, years	18–71	18–84	19–83	18–75
15 s **EEG Data**	2993	2898	2241	2224

histograms of these map signals have been utilized as the feature vector.

The steps below present the steps involved in creating the hypercube pattern.

Step 1: Create overlapping blocks with a length of 16 since we have used EEG signals, and our proposed pattern (hypercube pattern) is designed using a matrix with a size of 4 × 4.
Step 2: Transform each overlapping block into a matrix with a size of 4 × 4.
Step 3: Generated binary features (bits) by deploying our proposed hypercube pattern and signum function. The recommended hypercube pattern is shown in Fig. 3.

As shown in Fig. 3, the bit generation has mathematically been defined below.

Table 2
Channels used in this work.

No	Channel	No	Channel	No	Channel	No	Channel	No	Channel
1	FP1A1	8	CZA1	15	F8A1	22	T3T5	29	F4C4
2	FP2A2	9	P3A1	16	T3A1	23	T5O1	30	C4P4
3	F3A1	10	P4A2	17	T4A2	24	FP1F3	31	P4O2
4	F4A2	11	PZA2	18	T5A1	25	F3C3	32	FP2F8
5	FZA2	12	O1A1	19	T6A2	26	C3P3	33	F8T4
6	C3A1	13	O2A2	20	FP1F7	27	P3O1	34	T4T6
7	C4A2	14	F7A1	21	F7T3	28	P2P4	35	T6O2

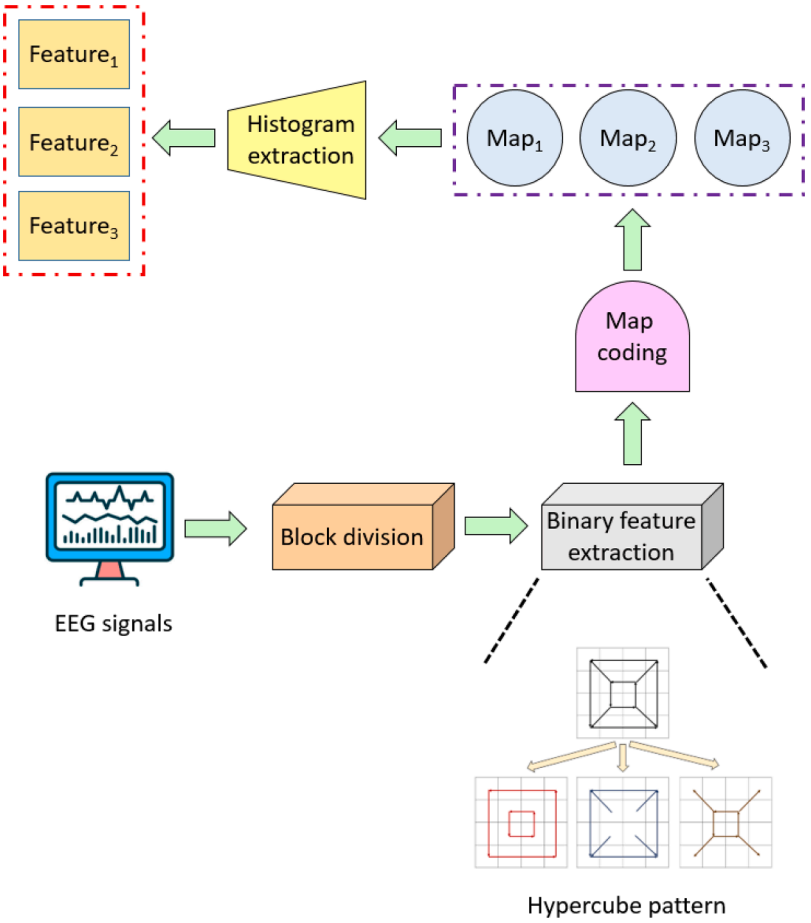

Fig. 2. Graphical overview of the hypercube pattern.
* Map_1: The feature signal generated by the first pattern, Map_2: feature signal created by the second pattern, Map_3: feature signal generated by the third pattern. By extracting the histogram of these maps, feature vectors have been created.

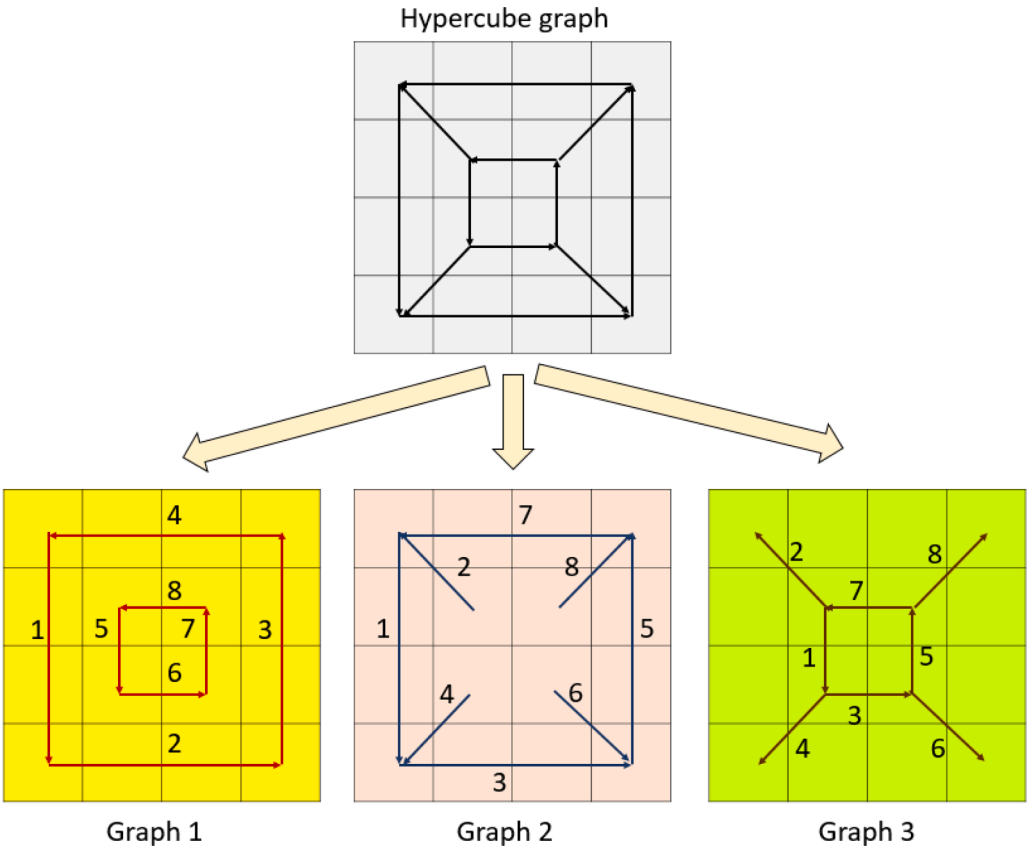

Fig. 3. Schematic diagram of the hypercube pattern used in this work. Three sub-graphs have been generated using the hypercube graph, and these graphs have eight edges. By using these edges, the binary patterns have been extracted. The edges have been demonstrated using arrows. Each arrow contains two data values. The initial point of the arrow depicts the first parameter and the finite point of the arrow demonstrates the second parameter. Also, enumerations of the bits are demonstrated using numbers with black font color. Using both values of the signum function, binary features (bits) have been generated and these bits have been utilized to get map signals to create three feature vectors.

$$\begin{vmatrix} b_1^1 & b_1^2 & b_1^3 \\ b_2^1 & b_2^2 & b_2^3 \\ b_3^1 & b_3^2 & b_3^3 \\ b_4^1 & b_4^2 & b_4^3 \\ b_5^1 & b_5^2 & b_5^3 \\ b_6^1 & b_6^2 & b_6^3 \\ b_7^1 & b_7^2 & b_7^3 \\ b_8^1 & b_8^2 & b_8^3 \end{vmatrix} = \sigma \begin{vmatrix} mt_{1,1}, mt_{4,1} \\ mt_{4,1}, mt_{4,4} \\ mt_{4,4}, mt_{1,4} \\ mt_{1,4}, mt_{1,1} \\ mt_{2,2}, mt_{3,2} \\ mt_{3,2}, mt_{3,3} \\ mt_{3,3}, mt_{2,3} \\ mt_{2,3}, mt_{2,2} \end{vmatrix}, \sigma \begin{vmatrix} mt_{1,1}, mt_{4,1} \\ mt_{2,2}, mt_{1,1} \\ mt_{4,1}, mt_{4,4} \\ mt_{3,2}, mt_{4,1} \\ mt_{4,4}, mt_{1,4} \\ mt_{3,3}, mt_{4,4} \\ mt_{1,4}, mt_{1,1} \\ mt_{2,3}, mt_{1,4} \end{vmatrix}, \sigma \begin{vmatrix} mt_{2,2}, mt_{3,2} \\ mt_{2,2}, mt_{1,1} \\ mt_{3,2}, mt_{3,3} \\ mt_{3,2}, mt_{4,1} \\ mt_{3,3}, mt_{2,3} \\ mt_{3,3}, mt_{4,4} \\ mt_{2,3}, mt_{2,2} \\ mt_{2,3}, mt_{1,4} \end{vmatrix} \quad (1)$$

$$\sigma\left(mt_{x1,y1}, mt_{x2,y2}\right) = \begin{cases} 0, mt_{x1,y1} - mt_{x2,y2} < 0 \\ 1, mt_{x1,y1} - mt_{x2,y2} \geq 0 \end{cases} \quad (2)$$

Herein, b defines bits (binary features), mt is the matrix created with a size of 4 × 4, and $\sigma(.,.)$ is the signum function. By deploying these functions (see Eqs. (1)-2), binary features have been created, and three types of bits have been generated from each overlapping block.

Step 4: Create three map signals by deploying binary to decimal transformation.

$$map_i^k = \sum_{j=1}^{8} b_j^k \times 2^{j-1}, \; i \in \{1, 2, \ldots, \mathscr{L} - 15\}, k \in \{1, 2, 3\} \quad (3)$$

Herein, *map* defines feature map signals, and $\mathscr{L}$ defines the length of the signal.

Step 5: Generate/extract histograms of the maps.

$$feat^k = \psi\left(map^k\right) \quad (4)$$

Herein, *feat* represents the feature vector, and the length of each feature vector is 256, $\psi(.)$ defines the histogram extraction function. The presented model generates three feature vectors.

2.3. The proposed hypercube pattern-based framework

In this work, we have recommended a fusion-based feature engineering model. In this model, we have used feature extraction combinations, and seven feature vectors have been obtained from each channel. The dataset used has 35 channels. Thus, the feature extraction phase has created 245 (=35 × 7) feature vectors. Furthermore, MDWT has been utilized to create multilevel feature creation. NCA chooses the most informative 256 features (we have chosen the most informative 256 features since one of the most popular feature generators, local binary pattern, extracts 256 features) and 245 (=7 × 35) feature vectors with a length of 256 have been created. The kNN classifier with LOSO CV was applied in the classification phase, and 245 results were obtained. IMV has been applied to fuse these results, and finally, the most accurate results are selected. The schematic overview of the recommended information fusion-based architecture is given in Fig. 4.

The phase-by-phase explanation has been given below to better explain the presented feature engineering model.

2.4. Feature extraction

We have used MDWT, hypercube pattern, and statistical feature extractors. Seven (=2^3–1 since the proposed hypercube pattern generates three feature vectors) feature vectors have been generated from each channel using combinations of these feature extractors. Since textural and statistical features have been merged, the recommended method is fused feature generation. For this point, we have presented (i)

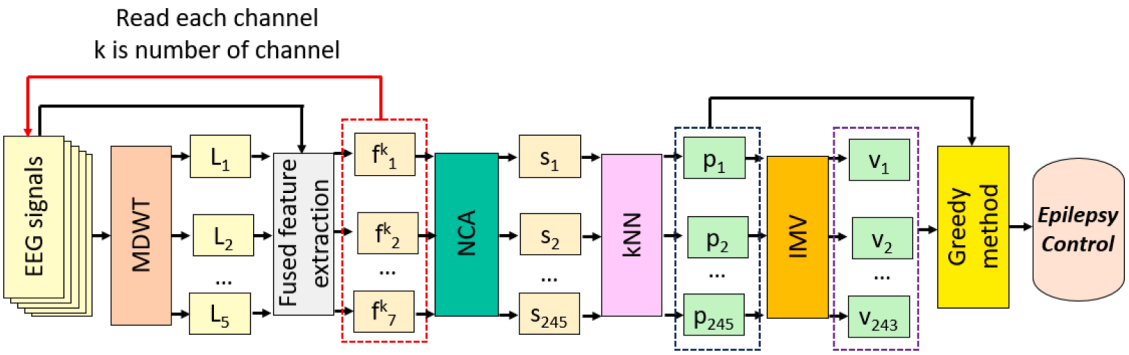

Fig. 4. Schematic overview of the proposed architecture.
The abbreviation used in this figure is explained as follows. *L: low-pass filter bands, f: feature vector, s: selected feature vector, p: predicted labels vectors, v: voted vectors.

multileveled, (ii) hybrid, and (iii) multiple domain-based feature extraction models in this research. The graphical explanation of our feature extraction method is depicted in Fig. 5.

A detailed explanation of our proposed combination-based feature extraction method is given in steps.

Step 1: Read each channel.
Step 2: The EEG signals are fed to the MDWT. We have used a sym4 filter and five-leveled MDWT since this combination is a commonly used noise reduction filter. In this phase, low-pass filters have been obtained. The used MDWT has mathematically been defined below.

$$[L_1, H_1] = \varphi(S)[L_{k+1}, H_{k+1}] = \varphi(L_k),\ k \in \{1, 2, \ldots, 4\} \tag{5}$$

where L implies low-pass filter bands, H defines high-pass filter bands, S is the raw EEG signal and $\varphi(.)$ is discrete wavelet transform.

Step 3: Extract features from low-pass filters and EEG signals by deploying a statistical feature extractor and the recommended hypercube pattern.

$$\begin{aligned} &\left[h_1^1\ h_2^1\ h_3^1\right] = \theta(S) \\ &\left[h_1^{t+1}\ h_2^{t+1}\ h_3^{t+1}\right] = \theta(L_t), t \in \{1, 2, \ldots, 5\} \\ &st^1 = \rho(S) \\ &st^{t+1} = \rho(L_t) \end{aligned} \tag{6}$$

where h represents features of the hypercube pattern, $\theta(.)$ defines the hypercube pattern feature generator, st is statistical features, and $\rho(.)$ represents statistical feature extraction. The used statistical features: maximum, mean, minimum, median, range, mode, standard deviation, variance, quartile range, energy, kurtosis, Tsallis entropy, Shannon entropy, wavelet entropy, sure entropy, log entropy, norm entropy, threshold entropy, root mean square and mean absolute deviation [48]. These 20 statistical moments have been employed for the raw input

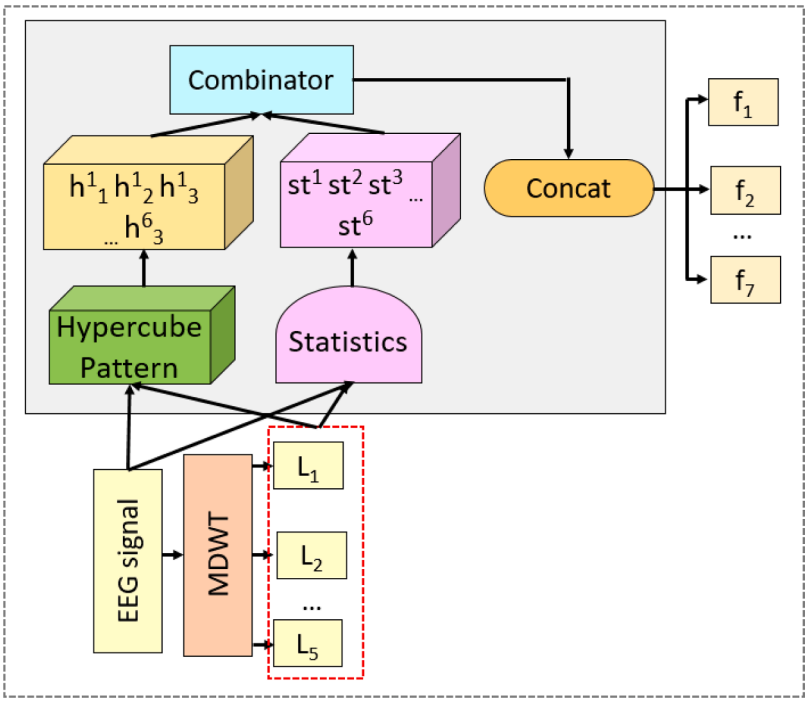

Fig. 5. Graphical overview of the suggested feature extraction method.
*h: textural feature by generating hypercube pattern, st: statistical features. The presented hypercube pattern generates three feature vectors, and we added the statistical features to these textural features extracted from the hypercube pattern. Thus, we generate 7 ($=2^3$–1) feature vectors for each channel.

signal and the absolute value of the input signal. Thus, $\rho(.)$ generates 40 features from a vector. Moreover, the length of each h is 256.

Step 4: Apply combinatory to generate seven feature vectors.

$$\begin{aligned} f^1 &= \mu\left(h_1^u, h_2^u, h_3^u, st^u\right), u \in \{1,2,\ldots,6\} \\ f^2 &= \mu\left(h_1^u, h_2^u, st^u\right) \\ f^3 &= \mu\left(h_1^u, h_3^u, st^u\right) \\ f^4 &= \mu\left(h_2^u, h_3^u, st^u\right) \\ f^5 &= \mu\left(h_1^u, st^u\right) \\ f^6 &= \mu\left(h_2^u, st^u\right) \\ f^7 &= \mu\left(h_3^u, st^u\right) \end{aligned} \tag{7}$$

where f means feature vectors and $\mu(.)$ is the concatenation function. In this step, seven feature vectors have been generated. The length of these feature vectors is given as follows. The length of f^1 is equal to 4848 (=(256+256+256+40) × 6), the lengths of f^2, f^3 and f^4 are equal. This length is 3312 (=(256+256+40) × 6), the length of the last three feature vectors (f^5, f^6, f^7) are equal, and the length of this feature is 1776 (=(256+40) × 6).

For each channel, seven feature vectors have been extracted. There are 35 channels in the used dataset. Therefore, this model generated 245 (=35 × 7) feature vectors.

2.5. Feature selection

We have generated 245 (=35 × 7) feature vectors with variable lengths in the fused feature extraction phase. In this phase, the most informative 256 features have been selected from each feature vector by deploying the NCA feature selector. NCA is similar to the kNN classifier since both algorithms have used distances to get results. We have used kNN classifier in the classification phase, and our essential objective is to use the advantage of the NCA and kNN couple. The graphical demonstration feature selection phase is depicted in Fig. 6.

Step 5 explains the NCA-based feature selection used.

Step 5: Apply NCA to choose the most informative 256 features.

$$\begin{aligned} in^r &= \phi(f^r, y),\ r \in \{1,2,\ldots,245\} \\ s^r(d,j) &= f^r(d, in^r(j)),\ d \in \{1,2,\ldots,dim\} \end{aligned} \tag{8}$$

where in^r indicates the sorted indexes, $\phi(.)$ defines the NCA feature selector, s means selected feature vectors, y is actual output, and dim defines the number of observations.

2.6. Classification

We have used kNN with LOSO CV to get the prediction vectors, and the selected features have been utilized as inputs of the kNN classifier. Our used dataset contains 121 subjects. Using LOSO CV, each subject has been utilized as a test, and others are used as training. This process is repeated 121 times, and each fold's calculated classification performance has been stored. In the final phase, the average classification performance of all folds has been calculated as the final classification performance for the LOSO CV. There are 245 selected feature vectors (the length of each feature vector is 256); hence, kNN generates 245 predicted vectors. The classification step of the proposed fusion-based architecture is depicted.

Step 6: Fed the features selected to kNN classifier with LOSO CV to get prediction vectors.

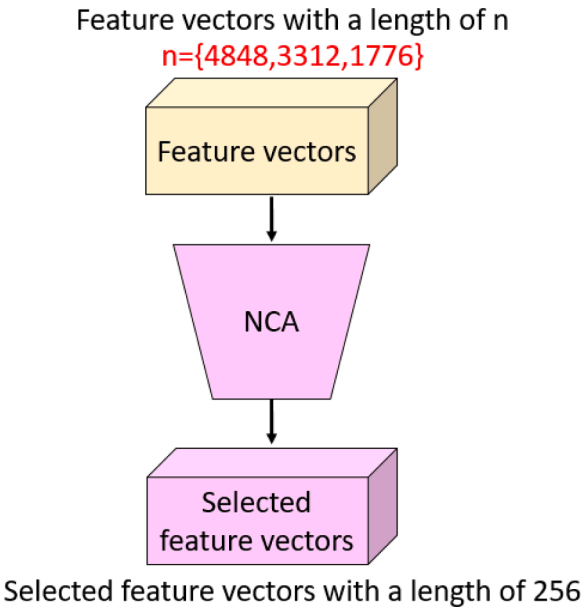

Fig. 6. Graphical representation of NCA-based feature selection.

$$p^r = \kappa(s^r, y) \tag{9}$$

where p defines the created prediction vectors by the kNN classifier and $\kappa(.)$ represents the support kNN classifier. The properties of the used kNN classifier have been given as follows. Here, k: 1, distance: L1-norm and voting: no.

2.7. Post-processing

Two basic algorithms have been used in this phase: IMV and greedy algorithms. IMV creates the voted vectors, and the greedy algorithm selects the best (the most accurate) predicted vector. IMV was recommended by Dogan et al. [49] in 2021. The loop range of the used IMV is from 3 to 245. Thus, 243 (=245–3 + 1) voted vectors have been created by deploying this iteration and mode function. The greedy algorithm selects the best-resulted vector per the maximum classification accuracy. The schematic overview of the recommended post-processing is shown in Fig. 7.

The steps of the post-processing phase are defined below.

Step 7: Create voted vectors by deploying IMV.

$$ac^r = \delta(p^r, y) i = \xi(ac) v^{r-2} = \omega\left(p^{i(1)}, p^{i(2)}, \ldots, p^{i(g)}\right),\ g \in \{3,4,\ldots,245\} \tag{10}$$

where $\delta(.)$ is the accuracy (ac) calculation function, $\xi(.)$ defines the sorting function, $\imath$ are the qualified indexes by descending per the classification accuracies and v represents voted vectors.

Step 8: Choose the maximum accurate vector by applying a greedy algorithm.

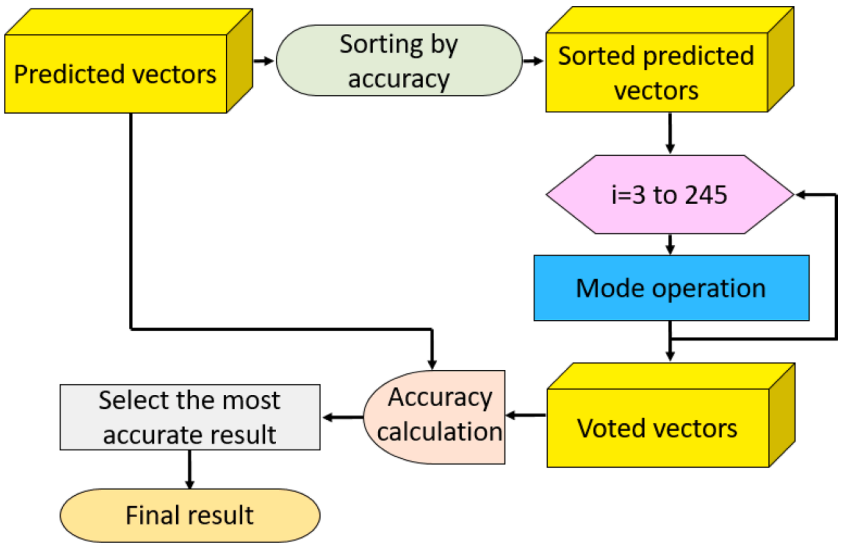

Fig. 7. Schematic illustration of the presented IMV and greedy algorithm-based post-processing method.

$$
\begin{aligned}
&ac^{r} = \delta(p^{r}, y)\\
&ac^{r+t} = \delta(v^{t}, y), t \in \{1, 2, \ldots, 243\}\\
&j = argmax(ac)\\
&fp = \begin{cases} p^{j},\ j \leq 245 \\ v^{j-245}, j > 245 \end{cases}
\end{aligned} \tag{11}
$$

Herein, j is the index of the best result, and fp defines the final predicted vector.

These eight steps given above have been defined in the presented architecture. Moreover, the indexes of the features and the used predicted vectors create an explainable model.

3. Experiments

We have proposed a fusion-based feature engineering model with a new hypercube pattern. Hypercube pattern is a textural feature extractor and generates three textural feature vectors. Furthermore, we have added these feature vectors to statistical features. In each channel, seven feature vectors have been generated. Thus, 245 feature vectors have been developed. The channel-wise results have been calculated, and the optimal model has been created in the post-processing phase. This model was implemented by MATLAB (2021a) programming environment was used for implementation. Moreover, other programming environments, for instance, python, can be used for implementation. The methods used to create this architecture are simple (they have linear complexities); hence, the presented architecture has a linear time burden.

3.1. Classification performance

The epilepsy dataset used has two classes (this problem is a binary classification problem). In this work, we have used six commonly used performance evaluation metrics: (i) classification accuracy, (ii) sensitivity/recall, (iii) specificity, (iv) precision, (v) F1-score, and (vi) geometric mean.

We have two types of results: voted and non-voted (single channel). The confusion matrices of these results are shown in Fig. 8.

Fig. 8 demonstrates that the best result belongs to the voted vectors, and this vector has been created using the top 74 prediction vectors. The best non-voted result belongs to the 25th channel (F3C3) and the feature

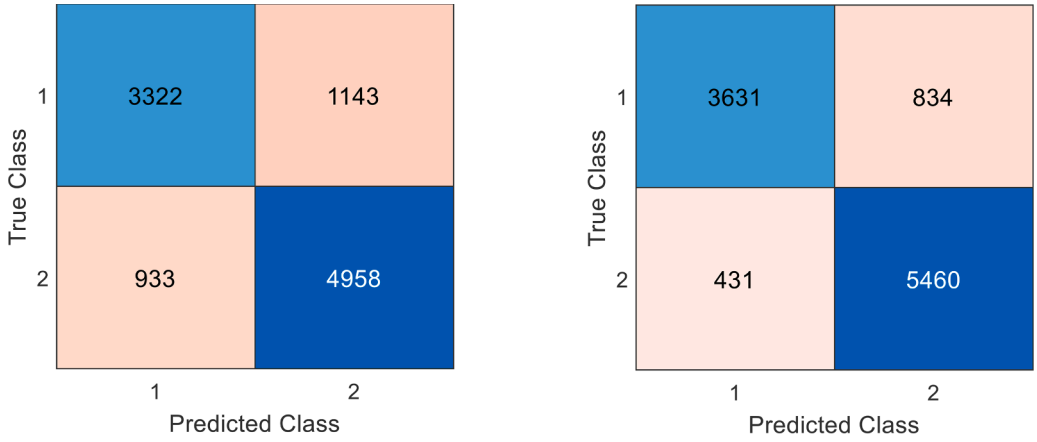

(a) Using non-voted vectors. (b) Using voted vectors.

Fig. 8. Confusion matrices obtained for the best feature vectors. *1: Epilepsy, 2: Control.

Table 3
Classification results (%) obtained for the proposed model using voted and non-voted vectors.

Metric	Non-voted	Voted
Accuracy(%)	79.95	87.78
Sensitivity(%)	74.40	81.32
Specificity(%)	84.16	92.68
Precision(%)	78.07	89.39
F1-score(%)	76.19	85.16
Geometric mean(%)	79.13	86.81

vector of this result is created by using the first and second features (f^2) of the hypercube pattern and statistical features. The classification performances of these results is shown in Table 3.

These results (see Table 3) demonstrated that our obtained the best result (voted vector) yielded over 80% for all classification performances with LOSO CV-based classification. Furthermore, our fused-based model reached 87.78% classification accuracy.

3.2. Explainable results

To give explainable results, we have presented channel-wise classification accuracies, the classification performances of the feature combination, feature distributions, and the effect of the used wavelet bands and the raw EEG signal for classification. Also, the number of prediction vectors needed to obtain optimal results is presented.

Epilepsy is a neurodegenerative disorder and affects some areas/lobes of the brain more than others. We have analyzed channel-wise classification accuracies to understand the epilepsy effect using our architecture. Therefore, boxplots of accuracies obtained for various channels are shown in Fig. 9.

Fig. 9 depicts that the best accurate channel is the 25th (F3C3) channel, and the average classification accuracy of this channel is 78.90%. Conversely, the least-performing channel to detect epilepsy using our model is the 32nd (FP2F8) channel since this channel's average classification accuracy is 61.10%.

We have generated seven feature vectors. The best accurate feature vector is the second feature vector on the 25th channel (see Fig. 8(a)). Moreover, we have shown the classification performances of these features in Fig. 10.

As can be seen from Fig. 10, the classification accuracies of these feature vectors are very close. The general classification accuracies (average ± standard deviation) of these feature vectors are tabulated in Table 4.

Table 4 highlighted that the maximum average classification accuracy belongs to the first feature vector and the first feature vector uses all three feature vectors of the hypercube pattern and statistical features. Also, the average classification accuracies of all feature vectors are higher than 70%.

We have used two types of feature vectors to create feature vectors. These are statistical and textural features. Our OEP-based models created 245 feature vectors selected. The average values of the number of selected features per feature type are also depicted in Fig. 11.

This figure (Fig. 11) demonstrates that the presented hypercube pattern features are more effective than statistical features in detecting epilepsy. However, statistical features have an effect on classification performance.

Raw EEG signals, L_1, L_2, L_3, L_4, and L_5 bands, have been used to generate feature vectors. NCA has chosen the top 256 features. The selected features in various bands and input signals are depicted in Fig. 12.

It can be noted from the figure that L_3 is the most useful one-dimensional signal for valuable feature generation.

The top 74 results were fused to get 87.78% classification accuracy, and the used feature vectors and channels are depicted in Fig. 13.

Fig. 13 highlighted that all features of the 5th (FZA2), 8th (CZA1), 11th (PZA2), 21st (F7T3), and 25th (F3C3) channels had been used to get the optimal results. Moreover, we have used 13 out of 35 channels to attain 87.78% classification accuracy. The results that f1 and f2 generate are the most used for creating the optimal model (see Fig. 13(b)).

4. Discussions

A big dataset consisting of 10,356 EEG signals acquired from 121 participants was used for this work. There are some bigger datasets than this dataset, but they are not epilepsy datasets. The temple university

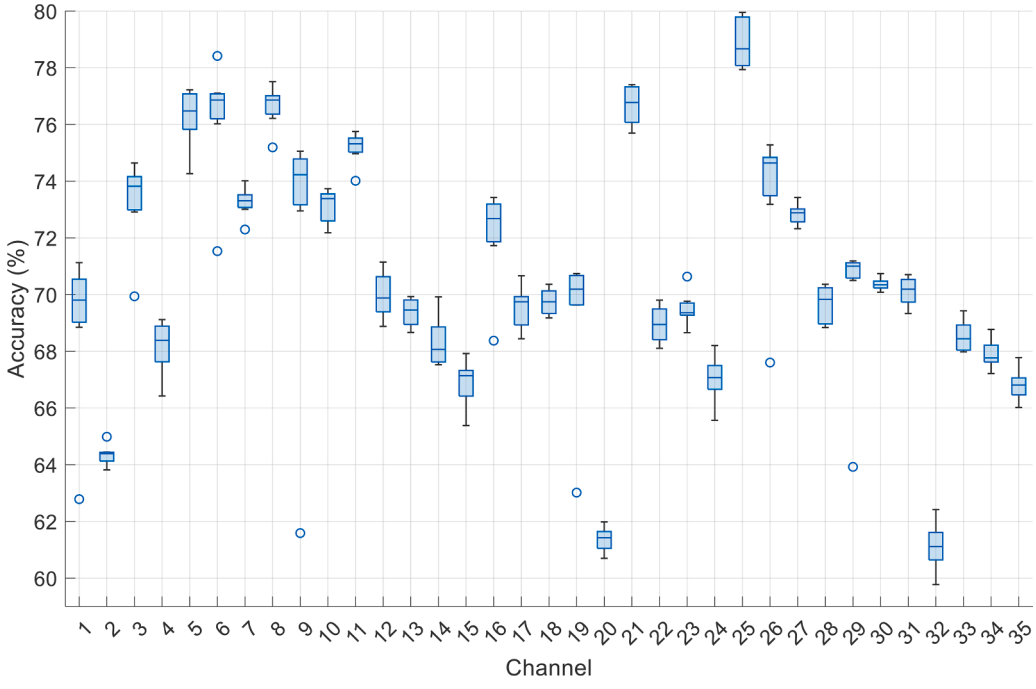

Fig. 9. Box plots showing the obtained accuracies for various channels.

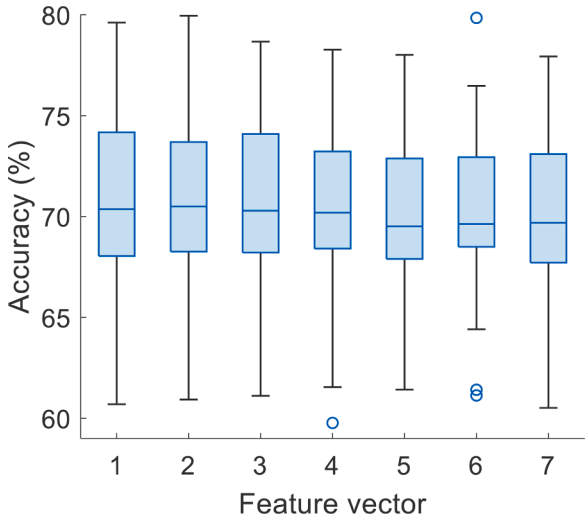

Fig. 10. Accuracies obtained for seven feature vectors.

Table 4
Classification accuracies obtained for seven feature vectors.

Feature vector	Accuracy (%)
f^1	70.88 ± 4.40
f^2	70.81 ± 4.28
f^3	70.72 ± 4.52
f^4	70.21 ± 4.46
f^5	70.13 ± 3.98
f^6	70.26 ± 4.14
f^7	70.22 ± 4.06

hospital (TUH) EEG dataset [50] has 28,000 EEG signals collected from 2002 to 2016. The TUH dataset has two classes: normal and abnormal. Abnormal can contain variable brain-related disorders, not only epilepsy. This is one of the biggest epileptic EEG datasets in the literature.

A new fusion-based explainable feature engineering model is presented in this work. Our model generated 488 vectors, 245 of them were non-voted, and 243 of them were voted. Our model is self-organized since the best accurate result is selected. The best classification accuracy is 87.78%, and this result belongs to voted vector. The calculated classification accuracies of these 488 vectors are depicted in Fig. 14.

Fig. 14 demonstrates that the information fusion algorithm – IMV – has improved the classification accuracy in the proposed model. The best classification accuracy of the non-voted is 79.95% and voted vectors range from 81.28% to 87.78%. Hence, the classification accuracy of our model was increased by 7.83% using the fusion model.

4.1. Comparative results

We have presented a new explainable and information fusion-based feature engineering architecture, and this model has been applied to a big EEG dataset by deploying LOSO CV. As a result, our model reached 87.78% classification accuracy with our private EEG dataset. Moreover, we have used the TUH dataset to demonstrate the high classification capability of our proposed explainable feature engineering model. The results obtained using the TUH dataset are shown in Fig. 15.

Fig. 15 shows the results obtained using our model using the TUH dataset. Our model attained 87.68% classification accuracy, 83.33% sensitivity, 91.33% specificity, 88.98% precision, 87.24% geometric mean, and 86.06% F1-score. Moreover, we have attained 86.23% classification accuracy using a single channel.

This justifies that our model is robust and accurate with huge databases. We have also compared our work with other state-of-the-art techniques in Table 5.

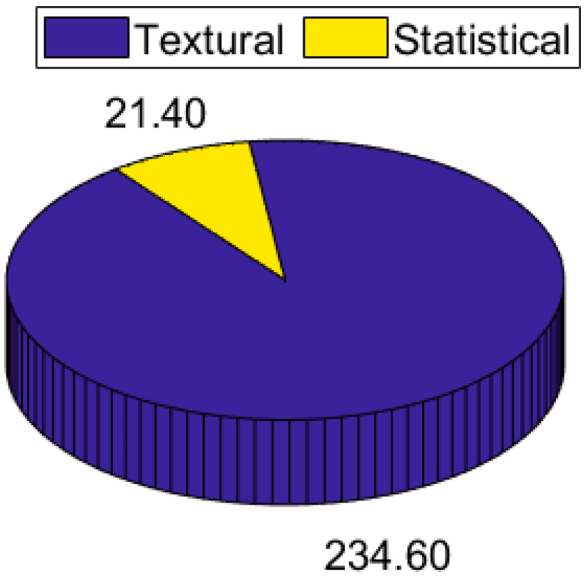

Fig. 11. Number of features used in two features.

Table 5 depicts that our hypercube pattern-based model reached satisfactory results. Moreover, we have used LOSO CV in the classification phase to create prediction vectors. Hence, our model yielded robust and accurate results. We have used the TUH dataset to get comparative results. Many deep learning-based EEG classification models have been used to get classification results using the TUH dataset. Our model is a feature engineering model and obtained higher classification performance than the listed models in Table 5. Moreover, the comparison results using the TUH dataset are shown in Fig. 16. This figure compares our model with ten popular CNN models.

The deep learning results shown in Fig. 16 were obtained from Raghu et al.'s study [59]. It may be noted from this figure that our model has obtained higher classification accuracy than ten deep learning models developed using the TUH dataset. Only the InceptionV3 model has yielded 0.62% higher (=88.30%) than our proposed model. Hence, we have presented a comparable model to deep learning models for EEG classification using the TUH dataset. Furthermore, we compared our model with EpilepsyNet [67] and EEGNet [68] using the TUH dataset. The obtained classification performances are presented in Fig. 17.

As shown in Fig. 17, we achieved a classification accuracy of 87.68% with our proposed feature engineering architecture. This performance is very close to the state-of-the-art EpilepsyNet, which achieved an accuracy of 88.04%. Additionally, our proposed model outperformed the

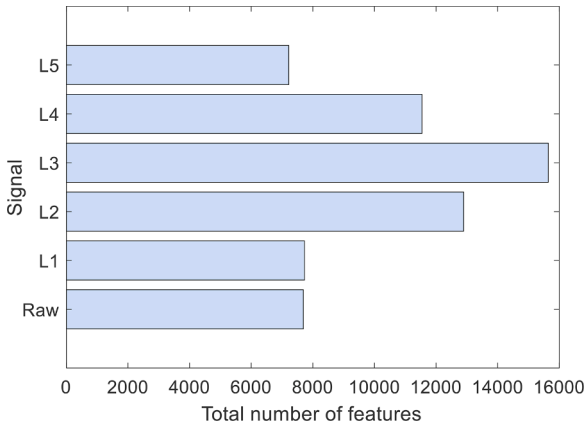

Fig. 12. Selected number of features in various bands and inputs.

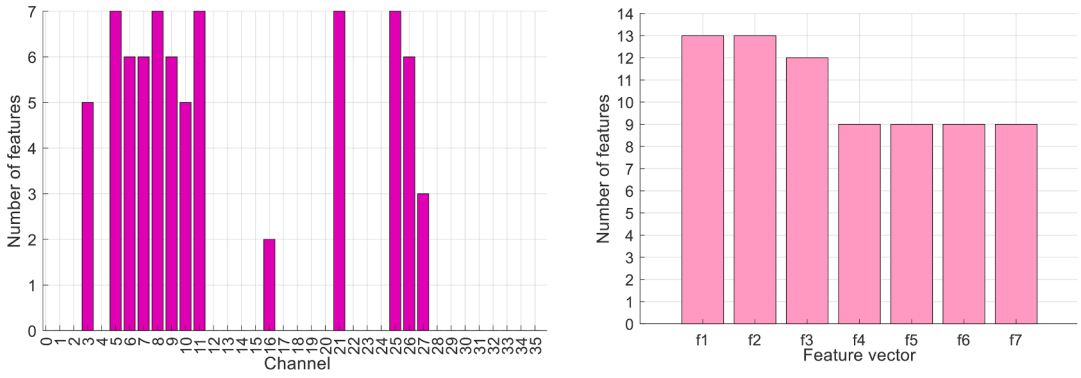

(a) Channels via a number of features (b) Number of features per the type of the features

Fig. 13. Number of features used per channel and feature type.

deep learning model EEGNet, which achieved an accuracy of 85.14%. These results demonstrate the competitiveness of our proposed feature engineering model with deep EEG models, including EpilepsyNet and EEGNet.

4.2. Ablations

We have used the 25th channel to give ablation results since this channel yielded the best results. The best combination for this channel is the first hypercube graph + the second hypercube graph + statistical moment. Moreover, MDWT and NCA were applied to get the feature vector in this combination. Herein, we presented three cases for ablations.

Case 1: First graph of the hypercube pattern to get features.
Case 2: The second graph of the hypercube has been used for feature generation.
Case 3: The third graph has been applied to get features.
Case 4: The statistical feature generator has been applied to create features.

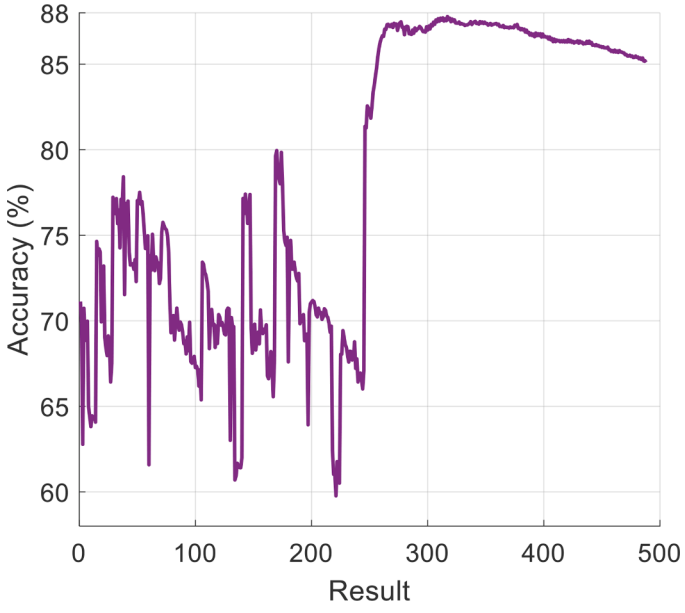

Fig. 14. Graph of classification accuracies versus the generated 488 prediction vectors.

The accuracies obtained in various cases and by our fused model are depicted in Fig. 18.

Fig. 18 shows that the proposed model has obtained the best classification performance.

4.3. Highlights

The most critical points of this model are given below.
Findings:

- A hypercube-based feature extraction model has been presented and is named the hypercube pattern.
- This model proposes a combination-based feature generation, and seven feature vectors have been created from each channel.
- The best-resulting feature vectors are f1 and f2. However, the general classification abilities of these feature vectors are very close.
- Channel-wise analysis has been conducted. In this work, the best resulting channel is the 25th channel.
- Our model generated 488 prediction vectors. 245 out of them were non-voted results, and 243 of them were voted results. Voted results have been created using the IMV algorithm.

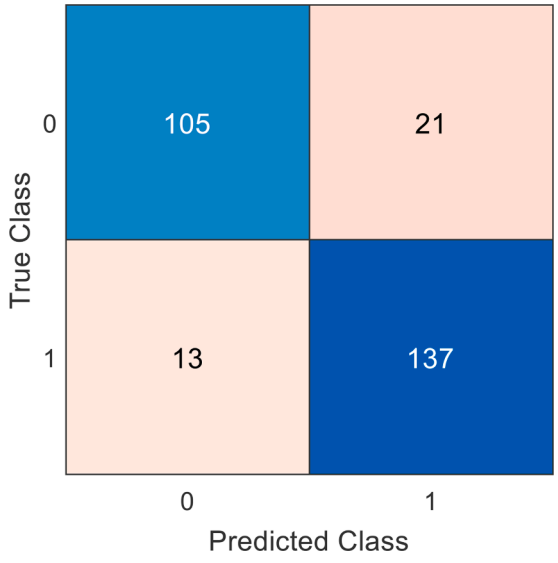

Fig. 15. Confusion matrix obtained using our proposed model for the TUH dataset. **0: Abnormal, 1: Normal.

Table 5
Summary of comparison of our work with other state-of-the-art methods developed using EEG signals.

Study	Method	Dataset	Split ratio	Results (%)
Islam et al. [51]	Dense convolutional blocks, Feature attention modules, Residual blocks, Hypercolumn technique	Bonn 500 single-channel EEG segments (each subset with a single duration of 23.6 s) every segment=4097 samples.) A: 5 healthy (eyes open) B: 5 healthy (eyes closed) C, D, E: Epilepsy patients	10 fold CV	Two class Accuracy=99.95 Three class Accuracy=99.98 Four class Accuracy=99.96 Five class Accuracy=99.96
Thomas et al. [52]	CNN, Template Matching, spectral feature-based classifier	Epileptic patients 33 patients (163 EEG signals) Nonepileptic patients 30 patients(44 EEG signals)	Leave-One-Institution-Out (LOIO) CV LOSO CV	LOIO CV AUC=0.826 Balanced Accuracy =76.1 LOSO CV AUC=0.812 Balanced Accuracy =74.8
Trangavel et al. [53]	1D ConvNet,2D ConvNet	554 subjects, 18,164 labeled IEDs 93 Epileptic EEGs 461 Nonepileptic EEGs	LOIO CV LOSO CV	LOIO CV AUC=0.839 Balanced Accuracy =78.10 LOSO CV AUC=0.856 Balanced Accuracy =79.5
Yang et al. [54]	Second quartile, kurtosis, skewness, mean, fuzzy entropy, Median, PFD, ApEn, SampEn, LZC	27 Epilepsy 17 Healthy	Leave-one-out CV	Accuracy=79.55 Recall=81.44 Specificity=76.47
Jing et al. [55]	DWT, Non-zero processing, SVM	Bonn 5 × 100 single-channel EEG segments (each subset with a single duration of 23.6 s) each segment=4096 samples.) A: 5 healthy (eyes open) B: 5 healthy (eyes closed) C, D, E: Epilepsy patients	10 fold CV	Accuracy=96.59 Specificity=97.39 Sensitivity=96.21
Wang et al. [56]	CNN, directed transfer function DTF	Freiburg 19 focal epilepsy patients (least 3 seizures) 82 seizures(459.1 h)	80:20	Sensitivity=90.80
Aristizabal et al. [57]	CNN, LSTM	1360 standard stimuli of 25 ms duration 240 deviant stimuli of 50 ms duration	5 fold CV	2D-CNN LSTM Accuracy=72.54
Liang et al. [58]	Long-Term recurrent convolutional network (LRCN)	23 patients (198 seizures) (916 hour)	LOSO CV	Accuracy=99.00 Sensitivity=84.00 Specificity=99.00
Raghu et al. [59]	Googlenet, Inceptionv3	TUH dataset 352 subjects	70:30	Googlenet Accuracy=82.85 Inceptionv3 Accuracy=88.30
Ma et al. [60]	Short-time Fourier transform, Vision Transformers	TUH dataset 675 subjects	63:25:12	AUROC: 92.10
Zhang et al. [61]	CNN	TUH dataset 14 subjects	LOSO CV	Accuracy: 80.50
Potter et al. [62]	Unsupervised variational autoencoder	TUH dataset	60:20:20	Accuracy: 83.00 Precision: 93.00 Recall: 86.00
Yildirim et al. [63]	1 dimensional CNN	TUH dataset	80:20	Accuracy: 79.34 Precision: 79.64 Recall: 78.71 F1: 78.92
Sharma et al. [64]	Localized wavelet filter banks	TUH dataset	10-fold CV	Accuracy: 79.34 Precision: 87.33 Recall: 77.54 F1-score: 88.14
Einizade et al. [65]	CNN, LSTM	TUH dataset	LOSO CV	Accuracy: 82.00 Sensitivity: 85.01 Specificity: 80.22 Precision: 71.69
Syamsundararao et al. [66]	CNN	TUH dataset	10-fold CV	Accuracy: 85.48 Precision: 76.65 Recall: 78.20 F1-score: 69.12

(*continued on next page*)

Table 5 (*continued*)

Study	Method	Dataset	Split ratio	Results (%)
Our Model	Hypercube, MDWT, NCA, kNN, IMV	Our collected dataset 50 Epilepsy 71 Healthy	LOSO CV	Non-Voted (single channel) Accuracy=79.95 Sensitivity=74.40 Specificity=84.16 Precision=78.07 F1-score=76.19 Voted Accuracy=87.78 Sensitivity=81.32 Specificity=92.68 Precision=89.39 F1-score=85.16
		TUH dataset	Training and testing separation	Non-Voted (single channel) Accuracy=86.23 Sensitivity=80.16 Specificity=91.33 Precision=88.60 F1-score=84.17 Voted Accuracy=87.68 Sensitivity=83.33 Specificity=91.33 Precision=88.98 F1-score=86.06

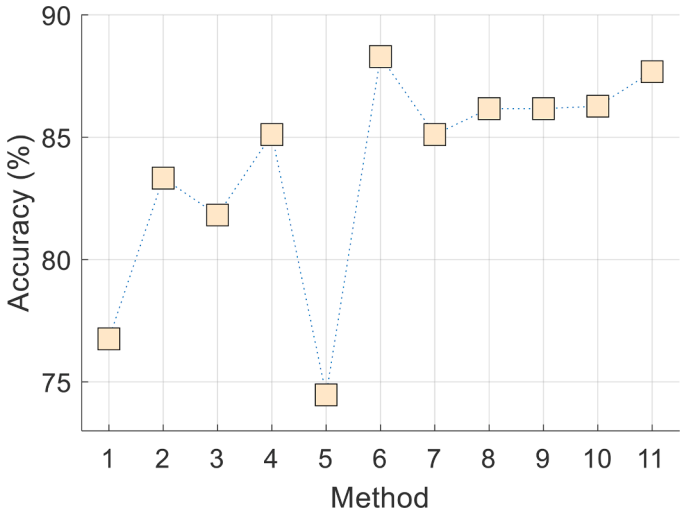

Fig. 16. Comparison of our accuracy obtained with ten other CNN models using the TUH dataset. **1: AlexNet, 2: Vgg16, 2: Vgg19, 4: SqueezeNet, 5: GoogLeNet, 6: InceptionV3, 7: DenseNet201, 8: Resnet18, 9: ResNet50, 10: ResNet101, 11: Our proposal.

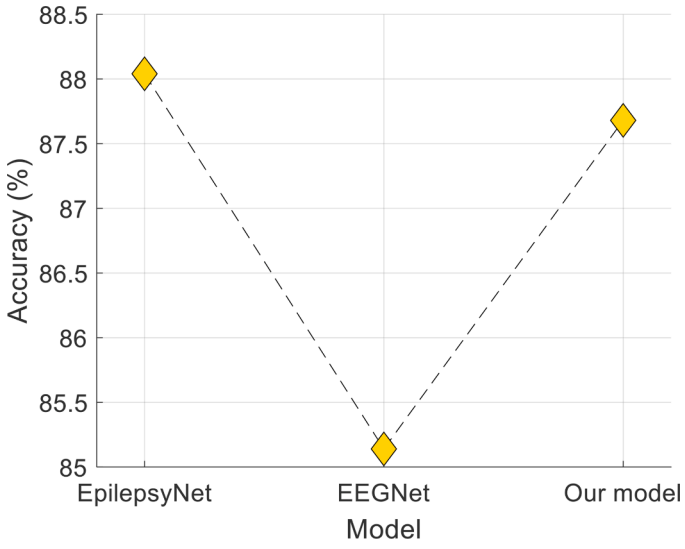

Fig. 17. Comparative results obtained using TUH dataset.

- The best classification ranges of the non-voted results ranged between 59.77% to 79.95%, while all voted results reached over 80% classification accuracies.
- 13 out of 35 channels have been used to attain optimal results.
- All feature vectors from the 5th, 8th, 11th, 21st, and 25th channels have been used to obtain 87.78% classification accuracy.
- The most effective signal for feature extraction is the L3 band.
- Two types of feature vectors: (i) textural and (ii) statistical, were extracted. The textural features contributed more to obtaining high performance.

The advantages of our proposed method are as follows:

- A combination-based feature extraction was proposed, and seven feature vectors were extracted from each channel.
- This model is handcrafted and the presented architecture is lightweight.
- A shallow classifier was used to get classification performances. Furthermore, LOSO CV has been used to validate results. By deploying LOSO CV, robust results were obtained.
- We have used a big dataset, and our model reached 87.78% classification performance on this corpus.
- Explainable results were presented in this work. Hence, this model is an explainable feature engineering model.
- The presented fusion-based feature engineering is a simple model for implementation.

Limitations of this work are given below:

- In the feature selection phase, we have used the NCA feature selector, but the iterative NCA is more effective than NCA. We can use

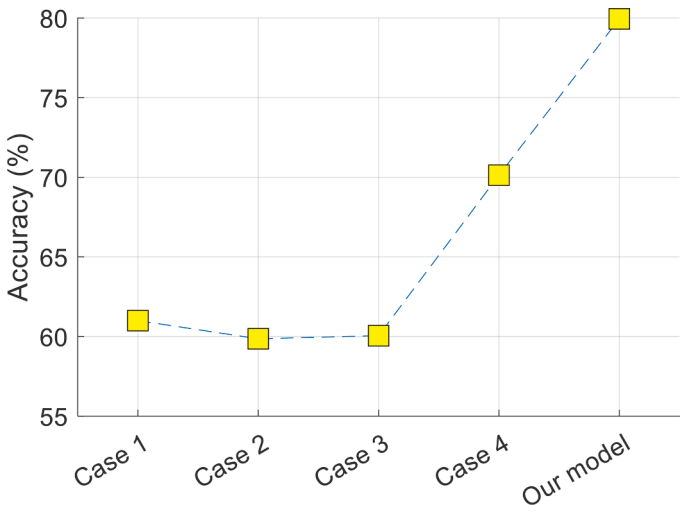

Fig. 18. Illustration of classification results due to the ablation study.

iterative NCA to get higher classification performance, but the computational complexity of the iterative NCA is high.

- Hyperparameter tuning can be applied to get higher performance. We have used methods with their default parameters. The optimized parameters can attain higher classification performances. Our proposed method is a parametric EEG classification architecture. The parameters (numbers) can be optimized for higher classification performance.
- A more diverse dataset can be used to improve the performance.

New generation and more effective combination-based explainable feature engineering models can be employed to handle these limitations [69].

5. Conclusion

Epilepsy is one of the most common neurological conditions worldwide. Therefore, an early, accurate diagnosis of this condition is crucial for optimal management. Therefore, automatic epilepsy detection using EEG signals has become a popular topic after developing advanced signal processing methods with machine learning models. However, the collected EEG signal datasets have been relatively small, and the classification performances of the machine learning models did not reflect reality due to small corpora. In this work, we collected a huge EEG dataset to solve this problem, and a new feature engineering model has been presented to get classification results on this corpus. Our objective is to present a combination/information fusion-based explainable to get high classification performance on the epilepsy data and explain epilepsy effects using our results. Our proposed method obtained an accuracy, sensitivity and specificity of 87.78%, 81.32%, and 92.68%, respectively, using our private dataset with the LOSO CV strategy. Also, using the TUG EEG corpus, our proposed model achieved an accuracy, sensitivity and specificity of 87.68%, 83.33% and 91.33%, respectively. It may be noted from Table 5 that we have obtained comparable results with state-of-the-art techniques developed using the TUH dataset. This justifies that our proposed hypercube pattern model is accurate and robust in detecting epilepsy using EEG signals. In the future, we intend to detect other neurological disorders like Alzheimer's disease, brain tumors, cerebral aneurysms, etc., using our model.

Funding

The authors state that this work has not received any funding.

Ethical approval

Malatya Turgut Ozal University (Turkey) Medical Faculty Ethics Committee (2022/01) approved the study.

CRediT authorship contribution statement

Irem Tasci: Conceptualization, Methodology, Validation, Investigation, Formal analysis, Resources, Data curation, Writing – original draft. **Burak Tasci:** Conceptualization, Methodology, Validation, Investigation, Writing – original draft, Writing – review & editing, Formal analysis, Resources, Data curation, Visualization. **Prabal D. Barua:** Conceptualization, Methodology, Validation, Investigation, Writing – original draft, Writing – review & editing, Formal analysis, Resources, Data curation, Visualization. **Sengul Dogan:** Conceptualization, Methodology, Validation, Investigation, Writing – original draft, Writing – review & editing, Software, Formal analysis, Resources, Data curation, Visualization. **Turker Tuncer:** Conceptualization, Methodology, Validation, Investigation, Writing – original draft, Writing – review & editing, Software, Formal analysis, Resources, Data curation, Visualization. **Elizabeth Emma Palmer:** Conceptualization, Validation, Investigation. **Hamido Fujita:** Conceptualization, Methodology, Validation, Investigation, Writing – original draft, Writing – review & editing. **U. Rajendra Acharya:** Conceptualization, Methodology, Validation, Investigation, Writing – original draft, Writing – review & editing, Supervision, Project administration.

Declaration of Competing Interest

The authors of this manuscript declare no conflicts of interest.

Data availability

This dataset is available in Kaggle and can be downloaded using https://www.kaggle.com/datasets/buraktaci/turkish-epilepsy URL.

References

[1] R. Thijs, R. Surges, T.J. O'brien, J.W. Sander, Epilepsy in adults, Lancet 393 (2019) 689–701.
[2] R.S. Fisher, C. Acevedo, A. Arzimanoglou, A. Bogacz, J.H. Cross, C.E. Elger, J. Engel Jr, L. Forsgren, J.A. French, M. Glynn, ILAE official report: a practical clinical definition of epilepsy, Epilepsia 55 (2014) 475–482.
[3] E. Wirrell, P. Tinuper, E. Perucca, S.L. Moshé, Introduction to the Epilepsy Syndrome Papers, Wiley Online Library, 2022, pp. 1330–1332.
[4] I.E. Scheffer, S. Berkovic, G. Capovilla, M.B. Connolly, J. French, L. Guilhoto, E. Hirsch, S. Jain, G.W. Mathern, S.L. Moshé, ILAE classification of the epilepsies: position paper of the ILAE commission for classification and terminology, Epilepsia 58 (2017) 512–521.
[5] Devinsky Orrin, Vezzani Annamaria, J. O'Brien Terence, S.I.E. Jette Nathalie, d. C. Marco, P. Piero, Epilepsy, Nat. Rev. Disease Primers 4 (2018) 1–24.
[6] L. Bättig, C. Dünner, D. Cserpan, A. Rüegger, C. Hagmann, B. Schmitt, F. Pisani, G. Ramantani, Levetiracetam versus Phenobarbital for Neonatal Seizures: a Retrospective Cohort Study, Pediatr. Neurol. 138 (2023) 62–70.
[7] E. YAVUZ, N. BEBEK, Epilepsi Tanı ve Tedavisinde Ektroensefalografinin (EEG) Yeri, Klinik Gelişim Dergisi (2010) 23.
[8] I.M. Shahwani, M.A. Dasti, M.A. Kalhoro, S. Ali, B. Waseem, S. Arwani, S.Z. A. Shah, Computed tomography (CT) Scan: ring enhancing lesions on brain, The Professional Med. J. 22 (2015) 321–326.
[9] A. Krumholz, S. Wiebe, G. Gronseth, S. Shinnar, P. Levisohn, T. Ting, J. Hopp, P. Shafer, H. Morris, L. Seiden, Practice parameter: evaluating an apparent unprovoked first seizure in adults (an evidence-based review):[RETIRED]: report of the quality standards subcommittee of the american academy of neurology and the American epilepsy society, Neurology 69 (2007) 1996–2007.
[10] M.A. King, M.R. Newton, G.D. Jackson, G.J. Fitt, L.A. Mitchell, M.J. Silvapulle, S. F. Berkovic, Epileptology of the first-seizure presentation: a clinical, electroencephalographic, and magnetic resonance imaging study of 300 consecutive patients, The Lancet 352 (1998) 1007–1011.
[11] S. Ramgopal, S. Thome-Souza, M. Jackson, N.E. Kadish, I.S. Fernández, J. Klehm, W. Bosl, C. Reinsberger, S. Schachter, T. Loddenkemper, Seizure detection, seizure prediction, and closed-loop warning systems in epilepsy, Epilepsy & Behav. 37 (2014) 291–307.

[12] A. Zayachkivsky, M.J. Lehmkuhle, J.J. Ekstrand, F.E. Dudek, Background suppression of electrical activity is a potential biomarker of subsequent brain injury in a rat model of neonatal hypoxia-ischemia, J. Neurophysiol. (2022).
[13] S.N.S. Kbah, N.K. Al-Qazzaz, S.H. Jaafer, M.K. Sabir, Epileptic EEG activity detection for children using entropy-based biomarkers, Neurosci. Inf. 2 (2022), 100101.
[14] W. Bauer, K.A. Dylag, A. Lysiak, W. Wieczorek-Stawinska, M. Pelc, M. Szmajda, R. Martinek, J. Zygarlicki, B. Bańdo, M. Stomal-Slowinska, Initial study on quantitative electroencephalographic analysis of bioelectrical activity of the brain of children with fetal alcohol spectrum disorders (FASD) without epilepsy, Sci. Rep. 13 (2023) 1–10.
[15] N.G. Seshadri, S. Agrawal, B.K. Singh, B. Geethanjali, V. Mahesh, R.B. Pachori, EEG based classification of children with learning disabilities using shallow and deep neural network, Biomed. Signal Process. Control 82 (2023), 104553.
[16] S. Poorani, P. Balasubramanie, Deep learning based epileptic seizure detection with EEG data, Int. J. Syst. Assurance Eng. Manag. (2023) 1–10.
[17] F. Hassan, S.F. Hussain, S.M. Qaisar, Fusion of multivariate EEG signals for schizophrenia detection using CNN and machine learning techniques, Inf. Fusion 92 (2023) 466–478.
[18] I. Assali, A.G. Blaiech, A.B. Abdallah, K.B. Khalifa, M. Carrère, M.H. Bedoui, CNN-based classification of epileptic states for seizure prediction using combined temporal and spectral features, Biomed. Signal Process. Control 82 (2023), 104519.
[19] D. Cimr, H. Fujita, H. Tomaskova, R. Cimler, A. Selamat, Automatic seizure detection by convolutional neural networks with computational complexity analysis, Comput. Methods Programs Biomed. 229 (2023), 107277.
[20] P. Sheoran, N. Rathee, J. Saini, Epileptic seizure detection using bidimensional empirical mode decomposition and distance metric learning on scalogram, in: 2020 7th International Conference on Signal Processing and Integrated Networks (SPIN), IEEE, 2020, pp. 675–680.
[21] S. JavadiMoghaddam, H. Gholamalinejad, A novel deep learning based method for COVID-19 detection from CT image, Biomed. Signal Process. Control 70 (2021), 102987.
[22] S.M. Usman, S. Khalid, S. Bashir, A deep learning based ensemble learning method for epileptic seizure prediction, Comput. Biol. Med. 136 (2021), 104710.
[23] S. Ryu, I. Joe, A hybrid DenseNet-LSTM model for epileptic seizure prediction, Appl. Sci. 11 (2021) 7661.
[24] A. Goshvarpour, A. Goshvarpour, Analytic representation vs. Angle modulation of hilbert transform of fast Walsh-Hadamard coefficients (HTFWHC) in epileptic EEG classification, Brazilian J. Phys. 53 (2023) 1–10.
[25] P. Khan, Y. Khan, S. Kumar, M.S. Khan, A.H. Gandomi, HVD-LSTM based recognition of epileptic seizures and normal human activity, Comput. Biol. Med. 136 (2021), 104684.
[26] S. Mishra, S. Kumar Satapathy, S.N. Mohanty, C.R. Pattnaik, A DM-ELM based classifier for EEG brain signal classification for epileptic seizure detection, Commun. Integr. Biol. 16 (2023), 2153648.
[27] M. Amiri, H. Aghaeinia, H.R. Amindavar, Automatic epileptic seizure detection in EEG signals using sparse common spatial pattern and adaptive short-time Fourier transform-based synchrosqueezing transform, Biomed. Signal Process. Control 79 (2023), 104022.
[28] M.Ravi Kumar, Y.Srinivasa Rao, Epileptic seizures classification in EEG signal based on semantic features and variational mode decomposition, Cluster Comput. 22 (2019) 13521–13531.
[29] A. Zarei, B.M. Asl, Automatic seizure detection using orthogonal matching pursuit, discrete wavelet transform, and entropy based features of EEG signals, Comput. Biol. Med. 131 (2021), 104250.
[30] M. Rashed-Al-Mahfuz, M.A. Moni, S. Uddin, S.A. Alyami, M.A. Summers, V. Eapen, A deep convolutional neural network method to detect seizures and characteristic frequencies using epileptic electroencephalogram (EEG) data, IEEE J. Transl. Eng. Health Med. 9 (2021) 1–12.
[31] M. Shen, P. Wen, B. Song, Y. Li, Real-time epilepsy seizure detection based on EEG using tunable-Q wavelet transform and convolutional neural network, Biomed. Signal Process. Control 82 (2023), 104566.
[32] Y. Zhao, D. Chu, J. He, M. Xue, W. Jia, F. Xu, Y. Zheng, Interactive local and global feature coupling for EEG-based epileptic seizure detection, Biomed. Signal Process. Control 81 (2023), 104441.
[33] X. Qiu, F. Yan, H. Liu, A difference attention ResNet-LSTM network for epileptic seizure detection using EEG signal, Biomed. Signal Process. Control 83 (2023), 104652.
[34] W.A. Mir, M. Anjum, S. Shahab, Deep-EEG: an optimized and robust framework and method for EEG-based diagnosis of epileptic seizure, Diagnostics 13 (2023) 773.
[35] J. Liu, P. Zhang, Q. Zou, J. Liang, Y. Chen, Y. Cai, S. Li, J. Li, J. Su, Q. Li, Status of epilepsy in the tropics: an overlooked perspective, Epilepsia Open (2023).
[36] H. Chovatiya, K. Yajnik, S. Desai, Prevalence of headache disorders in patients living with epilepsy in rural region in western part of India, Epilepsy & Behav. 139 (2023), 109063.
[37] X. Xu, Y. Zhang, R. Zhang, T. Xu, Patient-specific method for predicting epileptic seizures based on DRSN-GRU, Biomed. Signal Process. Control 81 (2023), 104449.
[38] F. Hassan, S.F. Hussain, S.M. Qaisar, Fusion of Multivariate EEG Signals for Schizophrenia Detection Using CNN and Machine Learning Techniques, Information Fusion, 2022.
[39] D. Hu, J. Cao, X. Lai, Y. Wang, S. Wang, Y. Ding, Epileptic state classification by fusing hand-crafted and deep learning EEG features, IEEE Trans. Circuits and Syst. II: Express Briefs 68 (2020) 1542–1546.
[40] G. Li, J.J. Jung, Deep Learning For Anomaly Detection in Multivariate Time Series: Approaches, Applications, and Challenges, Information Fusion, 2022.
[41] S.-H. Fang, W.H. Chang, Y. Tsao, H.C. Shih, C. Wang, Channel state reconstruction using multilevel discrete wavelet transform for improved fingerprinting-based indoor localization, IEEE Sens. J. 16 (2016) 7784–7791.
[42] S. Raghu, N. Sriraam, Classification of focal and non-focal EEG signals using neighborhood component analysis and machine learning algorithms, Expert Syst. Appl. 113 (2018) 18–32.
[43] L.E. Peterson, K-nearest neighbor, Scholarpedia, 4 (2009) 1883.
[44] R. Gupta, J. He, R. Ranjan, W.S. Gan, F. Klein, C. Schneiderwind, A. Neidhardt, K. Brandenburg, V. Välimäki, Augmented/mixed reality audio for hearables: sensing, control, and rendering, IEEE Signal Process. Mag. 39 (2022) 63–89.
[45] M. Okaba, T. Tuncer, An automated location detection method in multi-storey buildings using environmental sound classification based on a new center symmetric nonlinear pattern: cS-LBlock-Pat, Automation in Construction 125 (2021), 103645.
[46] A. Subasi, S. Dogan, T. Tuncer, A novel automated tower graph based ECG signal classification method with hexadecimal local adaptive binary pattern and deep learning, J. Ambient Intell. Humaniz. Comput. (2021) 1–15.
[47] Y. Cao, P. Cao, H. Chen, K.M. Kochendorfer, A.B. Trotter, W.L. Galanter, P. M. Arnold, R.K. Iyer, Predicting ICU admissions for hospitalized COVID-19 patients with a factor graph-based model. Multimodal AI in Healthcare, Springer, 2023, pp. 245–256.
[48] F. Kuncan, K. Yılmaz, M. Kuncan, Sensör Işaretlerinden Cinsiyet Tanıma Için Yerel Ikili örüntüler tabanlı Yeni Yaklaşımlar, 34, Gazi Üniversitesi Mühendislik Mimarlık Fakültesi Dergisi, 2019, pp. 2173–2186.
[49] A. Dogan, M. Akay, P.D. Barua, M. Baygin, S. Dogan, T. Tuncer, A.H. Dogru, U. R. Acharya, PrimePatNet87: prime pattern and tunable q-factor wavelet transform techniques for automated accurate EEG emotion recognition, Comput. Biol. Med. 138 (2021), 104867.
[50] I. Obeid, J. Picone, The temple university hospital EEG data corpus, Front. Neurosci. 10 (2016) 196.
[51] M.S. Islam, K. Thapa, S.H. Yang, Epileptic-net: an improved epileptic seizure detection system using dense convolutional block with attention network from EEG, Sensors 22 (2022) 728.
[52] J. Thomas, P. Thangavel, W.Y. Peh, J. Jing, R. Yuvaraj, S.S. Cash, R. Chaudhari, S. Karia, R. Rathakrishnan, V. Saini, Automated adult epilepsy diagnostic tool based on interictal scalp electroencephalogram characteristics: a six-center study, Int. J. Neural Syst. 31 (2021), 2050074.
[53] P. Thangavel, J. Thomas, W.Y. Peh, J. Jing, R. Yuvaraj, S.S. Cash, R. Chaudhari, S. Karia, R. Rathakrishnan, V. Saini, Time–frequency decomposition of scalp electroencephalograms improves deep learning-based epilepsy diagnosis, Int. J. Neural Syst. 31 (2021), 2150032.
[54] L. Yang, J. He, D. Liu, W. Zheng, Z. Song, EEG microstate features as an automatic recognition model of high-density epileptic EEG using support vector machine, Brain Sci. 12 (2022) 1731.
[55] J. Jing, X. Pang, Z. Pan, F. Fan, Z. Meng, Classification and identification of epileptic EEG signals based on signal enhancement, Biomed. Signal Process. Control 71 (2022), 103248.
[56] G. Wang, D. Wang, C. Du, K. Li, J. Zhang, Z. Liu, Y. Tao, M. Wang, Z. Cao, X. Yan, Seizure prediction using directed transfer function and convolution neural network on intracranial EEG, IEEE Trans. Neural Syst. Rehabilitation Eng. 28 (2020) 2711–2720.
[57] D. Ahmedt-Aristizabal, T. Fernando, S. Denman, J.E. Robinson, S. Sridharan, P. J. Johnston, K.R. Laurens, C. Fookes, Identification of children at risk of schizophrenia via deep learning and EEG responses, IEEE J. Biomed. Health Inform. 25 (2020) 69–76.
[58] W. Liang, H. Pei, Q. Cai, Y. Wang, Scalp EEG epileptogenic zone recognition and localization based on long-term recurrent convolutional network, Neurocomputing 396 (2020) 569–576.
[59] S. Raghu, N. Sriraam, Y. Temel, S.V. Rao, P.L. Kubben, EEG based multi-class seizure type classification using convolutional neural network and transfer learning, Neural Networks 124 (2020) 202–212.
[60] Y. Ma, C. Liu, M.S. Ma, Y. Yang, N.D. Truong, K. Kothur, A. Nikpour, O. Kavehei, TSD: Transformers for Seizure Detection, bioRxiv, 2023, 525308, 2023.2001. 2024.
[61] X. Zhang, L. Yao, M. Dong, Z. Liu, Y. Zhang, Y. Li, Adversarial representation learning for robust patient-independent epileptic seizure detection, IEEE J. Biomed. Health Inform. 24 (2020) 2852–2859.
[62] İ.Y. Potter, G. Zerveas, C. Eickhoff, D. Duncan, Unsupervised Multivariate Time-Series Transformers for Seizure Identification On EEG, arXiv preprint, 2023. arXiv:2301.03470.
[63] Ö. Yıldırım, U.B. Baloglu, U.R. Acharya, A deep convolutional neural network model for automated identification of abnormal EEG signals, Neural Comput. App. 32 (2020) 15857–15868.
[64] M. Sharma, S. Patel, U.R. Acharya, Automated detection of abnormal EEG signals using localized wavelet filter banks, Pattern Recognit. Lett. 133 (2020) 188–194.
[65] A. Einizade, M. Mozafari, S.H. Sardouie, S. Nasiri, G. Clifford, A deep learning-based method for automatic detection of epileptic seizure in a dataset with both generalized and focal seizure types, in: 2020 IEEE Signal Processing in Medicine and Biology Symposium (SPMB), IEEE, 2020, pp. 1–6.
[66] T. Syamsundararao, A. Selvarani, R. Rathi, N.V.A. Grace, D. Selvaraj, K. M. Almutairi, W.B. Alonazi, K. Priyan, R. Mosissa, An efficient signal processing algorithm for detecting abnormalities in EEG signal using CNN, Contrast Media Mol. Imaging (2022) 2022.

[67] A. Lebal, A. Moussaoui, A. Rezgui, Epilepsy-Net: Attention-Based 1D-Inception Network Model For Epilepsy Detection Using One-Channel and Multi-Channel EEG Signals, Multimedia Tools and Applications, 2022, pp. 1–23.
[68] V.J. Lawhern, A.J. Solon, N.R. Waytowich, S.M. Gordon, C.P. Hung, B.J. Lance, EEGNet: a compact convolutional neural network for EEG-based brain–computer interfaces, J. Neural Eng. 15 (2018), 056013.
[69] H.W. Loh, C.P. Ooi, S. Seoni, P.D. Barua, F. Molinari, U.R. Acharya, Application of explainable artificial intelligence for healthcare: a systematic review of the last decade (2011–2022), Comput. Methods Programs Biomed. (2022), 107161.